Journal of the European Ceramic Society **13** (1994) 53–60

Thermal Stability of Electroconductive TiN-Reinforced Silicon Oxynitride Composites

W. Lin* & J.-M. Yang

Department of Materials Science & Engineering, University of California, Los Angeles, California 90024-1595, USA

(Received November 1992; revised version received 9 August 1993; accepted 23 August 1993)

Abstract

The thermal stability and oxidation behavior of TiN-reinforced silicon oxynitride (Si_2N_2O) composites with different sintering additives fabricated by in-situ reaction forming process was investigated at temperatures ranging from 950 to 1400°C in air. The oxide scale was characterized by X-ray diffraction, scanning electron microscopy and electron probe microanalysis. The influence of sintering additives on the oxidation kinetics and rate-controlling mechanisms was also investigated. The thermal stability of these TiN-reinforced Si_2N_2O composites was found to be dominated by the oxidation of TiN phase.

Die thermische Stabilität und das Oxidationsverhalten von TiN-verstärkten Siliziumoxynitrid (Si_2N_2O) Kompositen mit verschiedenen Sinterzusätzen und hergestellt durch in-situ Reaktionsformpressen wurde für einen Temperaturbereich von 950–1400°C in Luftatmosphäre untersucht. Die Oxidationsschicht wurde mit Hilfe von Röntgenbeugung, Rasterelektronenmikroskopie und Elektronensonde charakterisiert. Der Einfluß der Sinterzusätze auf die Oxidationskinetik und den Raten bestimmenden Mechanismus wurde ebenso untersucht. Es zeigte sich, daß die thermische Stabilität dieser TiN-verstärkten Si_2N_2O-Komposite durch die Oxidation der TiN-Phase bestimmt wird.

On a étudié la stabilité et l'oxydation, sous air, entre 950° et 1400°C, de composites d'oxynitrure de silicium (Si_2N_2O) renforçés par TiN; ces composites comportent différents additifs de frittage et sont fabriqués par un procédé de formage réactionnel. La couche d'oxyde a été caractérisée par diffraction de rayons X, microscopie à balayage et microsonde de Castaing. On s'est également intéressé à l'influence des additifs de frittage sur la cinétique d'oxydation et sur ses mécanismes. La stabilité de ces composites de Si_2N_2O renforçés par TiN semble contrôlée par l'oxydation de TiN.

1 Introduction

Silicon oxynitride (Si_2N_2O) is a promising engineering ceramic for high temperature structural applications. It has been shown that Si_2N_2O exhibits no degradation of flexural strength up to 1300°C.[1] The oxidation resistance is also reported to be superior to that of silicon nitride and silicon carbide up to 1750°C.[2,3] However, like other engineering ceramics such as Si_3N_4 and SiC, the relatively low toughness (2–4 MPa $m^{1/2}$) of Si_2N_2O is the major limiting factor for structural applications.

The need of decreasing the flaw-sensitivity and increasing the damage tolerance of ceramics have led to the development of composites. Various particulates, whiskers and continuous fibers have been incorporated into monolithic ceramics to improve the strength and fracture toughness.[4–6] Recently, increasing attention has also been placed in developing composites with electrically conductive second phases, such as TiN, TiC or TiB_2.[7–9] It has been shown that the addition of the conductive second phases improves not only the fracture toughness and strength[10,11] but also the electrical conductivity of the composite. This enables the use of electrical discharge machining for manufacturing the components with complex shapes.[12]

The feasibility of developing an electroconductive TiN-reinforced silicon nitride/silicon oxynitride composite using an in-situ TiN forming technique has been demonstrated in an earlier paper.[13] This work was conducted to study the thermal stability and oxidation resistance of the TiN/Si_2N_2O com-

* Present address: Center for Aviation and Space Technology, Industrial Technology Research Institute, Hsinchu, Taiwan.

Journal of the European Ceramic Society 0955-2219/94/$7.00

posites in air. The effect of sintering additives on the oxidation kinetics as well as the morphology of oxide scale were also discussed.

2 Experimental Procedure

2.1 Materials and processing

Composites with different sintering additives, denoted as Si/4/0 (4 wt% of Y_2O_3 and 0 wt% of Al_2O_3) and Si/6/3 (6 wt% of Y_2O_3 and 3 wt% of Al_2O_3), were prepared by reaction bonding and then hot pressing of Si (with sintering additives) + 60 wt% of TiO_2 powder mixture. Commercial Si powder (Kema Nord), TiO_2 powder (J. T. Baker), Al_2O_3 powder (Alcoa) and Y_2O_3 powder (Molycorp) were used as the raw materials. The powders were carefully weighed and wet milled with pure Si_3N_4 medium in Neoprene/isopropyl alcohol solution for 24 h. The homogenization is obtained through a pH control method by adding OH^-. The mixed slurry was then dried in air followed by a dry milling (0·5 h) and screening (30 mesh) to break the 'cake' formed during drying and also to prevent the agglomeration. The powder mixtures were cold pressed into a $15 \times 15 \times 2{\cdot}5\,cm^3$ plate under a pressure of 5–7 MPa at room temperature and then nitrided at 1100–1400°C for 192 h, followed by hot pressing at 1750°C, 24 MPa in nitrogen atmosphere for 3 h. The results of XRD analysis of hot-pressed specimens showed that Si and TiO_2 had been completely converted to Si_2N_2O and TiN, respectively. No crystalline intergranular phases was detected in the Si/6/3 composites, while β-$Y_2Si_2O_7$ was identified as a crystalline intergranular phase for Si/4/0 specimen.[13] A detailed description of the effect of sintering additives on microstructural development of these composites can be found in Ref. 13.

2.2 Oxidation tests and analysis

Specimens with a size of $2 \times 12 \times 25$ mm were cut from the hot-pressed billets, wet-polished with various grade of diamond paste down to 1 μm, and then ultrasonically cleaned in acetone. Long-term oxidation tests (up to 175 h) were conducted at temperatures ranging from 950 to 1400°C in air. The isothermal weight gain was recorded at different exposure times. After the oxidation test, the oxide scale formed at different temperatures were analyzed by X-ray diffraction (XRD), scanning electron microscopy (SEM) with EDS and electron-probe microanalysis (EMPA).

3. Results and Discussion

3.1 TiN-reinforced Si/4/0 composite

The oxidation behavior of TiN-reinforced Si/4/0 composite at temperatures ranging from 950 to 1400°C in air is shown in Fig. 1. The weight gain per unit area, $\Delta W/A$, was found to increase parabolically with time over the entire temperature range. Figure 2 shows the replot of these data in terms of the parabolic form (squares of the weight gain per unit area versus time). It is obvious that all the data fit into different straight lines except those at 1400°C for $t > 20$ h. This suggests a classic parabolic oxidation behavior, which can be represented by the equation:

$$(\Delta W/A)^2 = k_p t$$

where ΔW is the weight gain at time t, A is the total surface area, and k_p is the parabolic rate constant. It should be noted that this equation is valid only if the surface area remains constant with time.

Figure 3 shows the plot of the parabolic rate constant, which was determined from the slopes of

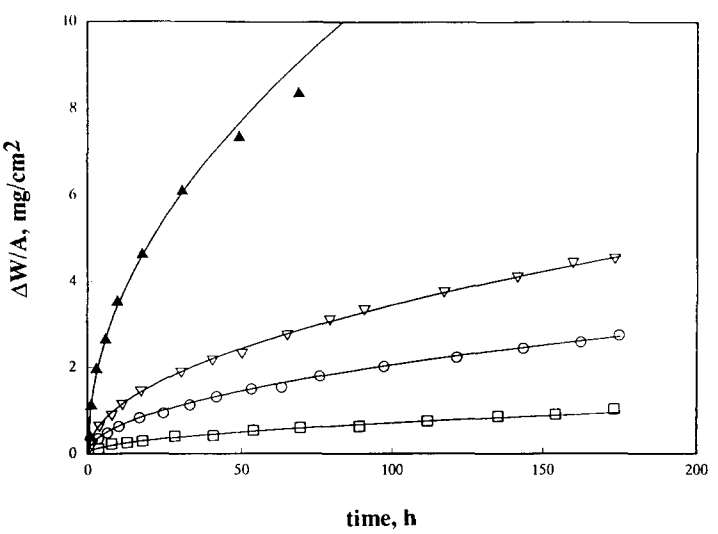

Fig. 1. Weight gain of TiN-reinforced Si/4/0 composite oxidized at various temperatures in air. □, 950°C; ○, 1100°C; ▽, 1250°C; ▲, 1400°C.

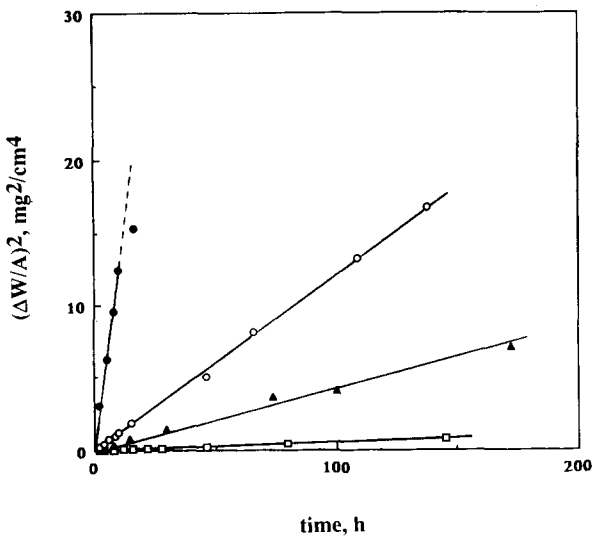

Fig. 2. Parabolic plot of weight change for TiN-reinforced Si/4/0 composite oxidized at various temperatures in air. □, 950°C; ▲, 1100°C; ○, 1250°C; ●, 1400°C.

the straight lines in Fig. 2, versus $1/T$. A linear relationship was found over the entire temperature range, i.e. 950–1400°C. This indicates that only one oxidation mechanism is active up to 1400°C. Figure 4 shows the surface morphologies of TiN-reinforced Si/4/0 material exposed at different temperatures in air for 175 h as revealed by SEM. It is clear that the surfaces of all the specimens were covered by rod- or plate-like crystallites and the size of these crystallites increases as the exposure temperature increases.

These crystallites were identified as titanium dioxide (rutile structure) by X-ray diffraction analysis. Also, severe cracking of the oxide scale was observed at temperatures above 1100°C. The cracking is believed to be induced by the mismatch in thermal expansion coefficient between the oxide

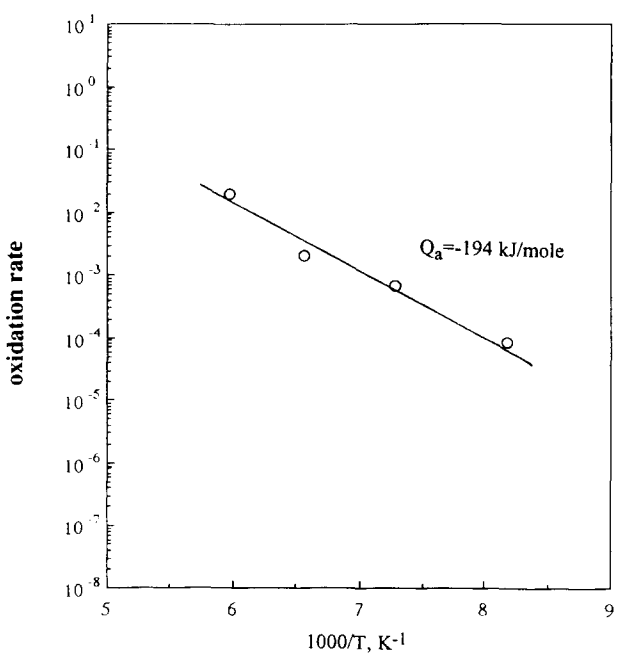

Fig. 3. Arrhenius plot of oxidation rate constant for TiN-reinforced Si/4/0 composites in air.

scale and Si_2N_2O. The results of X-ray diffraction analysis also indicated that the TiO_2 scale had preferred orientation on (101) for $T \leq 1100°C$ and (110) for $T \geq 1250°C$, as shown in Fig. 5. These TiO_2 crystallites appear to be formed by the oxidation of TiN through the following reaction:

$$TiN + O_2 \rightarrow TiO_2 + 1/2N_2 \quad (1)$$

SEM examination of the surface morphology of the TiN-reinforced Si/4/0 composite exposed at 1250°C for 0·5 h showed that, in addition to TiO_2 crystallites, a silica film was observed covering the surface of the specimen. Cracking of the oxide scale due to the mismatch in thermal expansion between the oxide scale and Si_2N_2O was observed. This SiO_2 film is believed to be produced by the reaction of silicon oxynitride with oxygen during the very early stage of oxidation. However, at this temperature, the oxidation of Si_2N_2O is not active. The silica layer remained very thin and an effective diffusion barrier was not activated. The further oxidation is thus considered as a selective oxidation process in which the TiN phase was selectively oxidized into TiO_2. This agrees well with the results of Bellosi *et al.*[14] and Mukerji & Biswas[15] on the oxidation of TiN–Si_3N_4 and TiN–Al_2O_3 composites, respectively, in which the oxidation of TiN is thought to be the governing reaction for the oxidation resistance of both composites.

The oxidation of TiN in TiN-reinforced Si_2N_2O composites may occur through the following two routes. One is the outward diffusion of Ti ions through the TiO_2 layer where the reaction occurs at the surface of outer TiO_2 layer. The other is the inward diffusion of oxygen through the TiO_2 layer where the reaction occurs at the interface between oxide scale and TiN-depleted zone. Figure 6 shows the back-scattered electron image (BEI) of a cross-section of the TiN-reinforced Si/4/0 composite oxidized at 1100°C for 175 h. Three distinct zones were clearly observed:

(a) External oxide scale which contains mainly titanium dioxide (rutile);
(b) porous TiN-depleted layer which contains basically the same microstructure as the bulk material with less TiN phase (bright spots);
(c) bulk material.

The same reaction zones were observed for specimens exposed at 1250, 1325 and 1400°C. The presence of this porous, TiN-depleted layer between the oxide scale and bulk material indicates that the outward diffusion of Ti ions to the oxide scale is faster than the inward diffusion of oxygen. Thus, the oxidation reaction should occur at either the surface of outer TiO_2 scale or the interface between the outer TiO_2 layer and TiN-depleted zone.

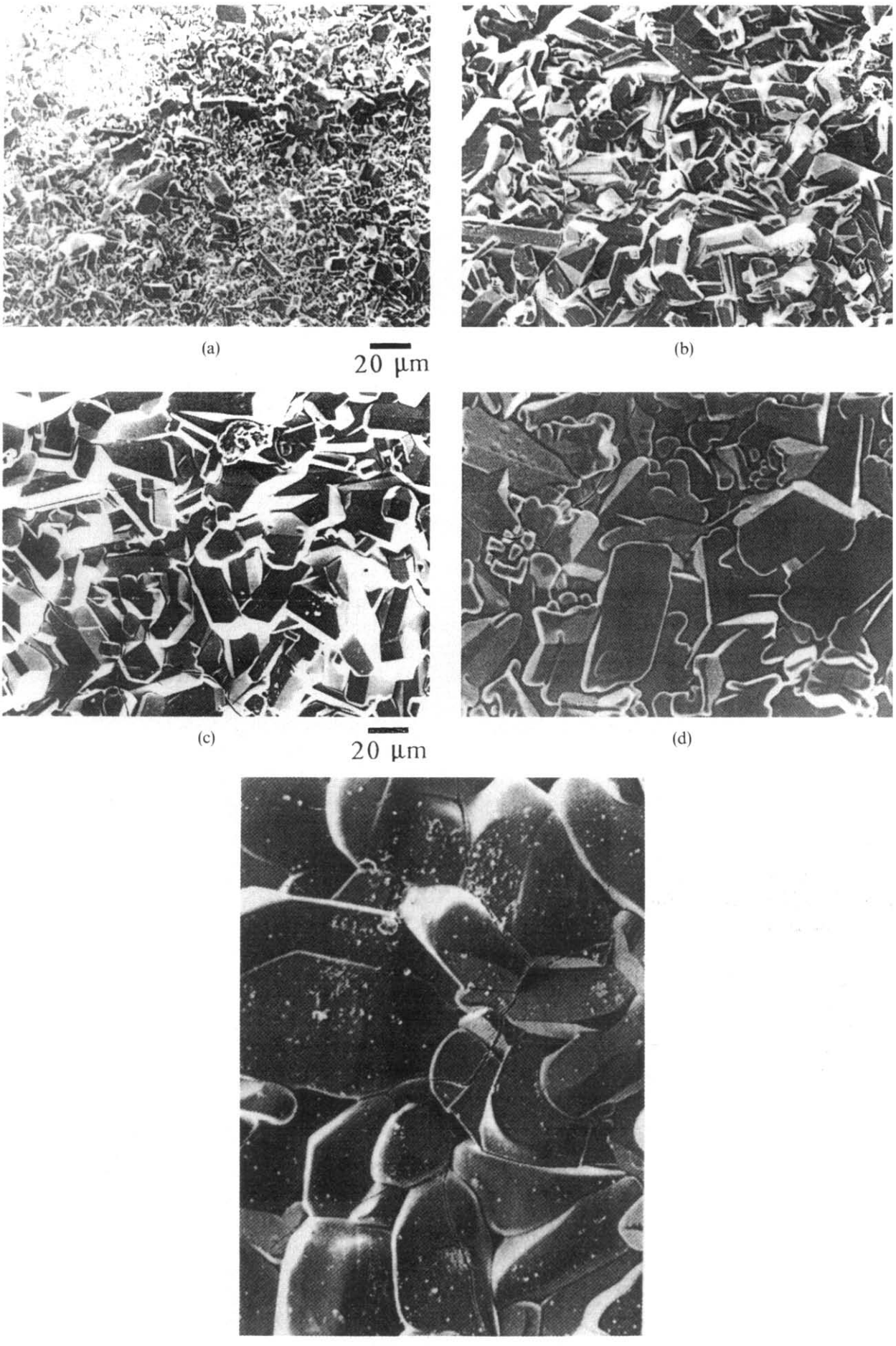

Fig. 4. Surface morphologies of TiN-reinforced Si/4/0 composite exposed at (a) 950, (b) 1100, (c) 1250, (d) 1325 and (e) 1400°C in air for 175 h.

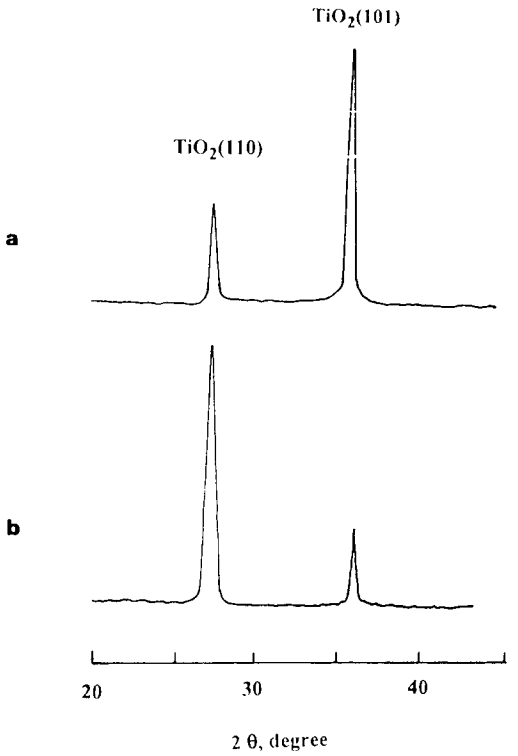

Fig. 5. X-Ray diffraction patterns of the oxide scale for TiN-reinforced Si/4/0 composite exposed at (a) 1100 and (b) 1250°C in air for 175 h.

The activation energy can be used to gain insight of the predominant mechanism that governs the oxidation behavior. An activation energy of 194 kJ/mol was calculated from Fig. 3. This value is very close to that (192 kJ/mol) reported by Munster & Schlamp[16] and Jenkins[17] for the oxidation of TiN and titanium alloys for which the inward diffusion of oxygen through the TiO_2 (rutile) layer is the oxidation rate-controlling mechanism. Moreover,

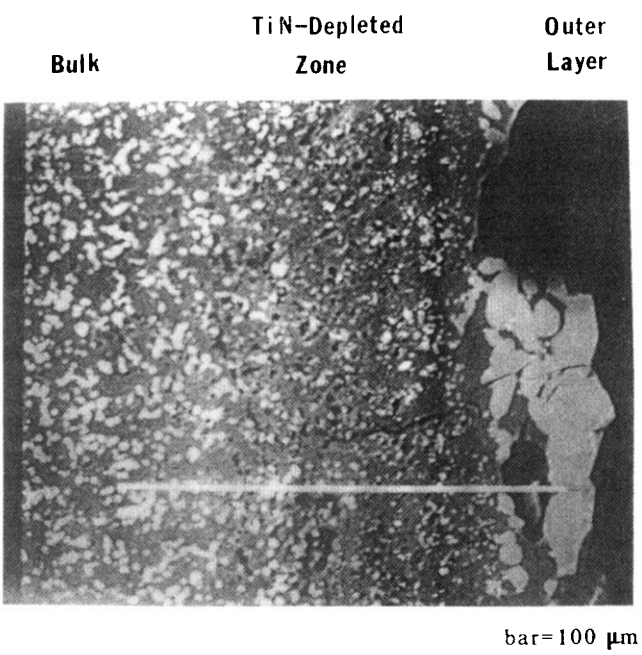

Fig. 6. The back-scattered electron image (BEI) of a transverse section of the TiN-reinforced Si/4/0 composite oxidized at 1100°C for 175 h.

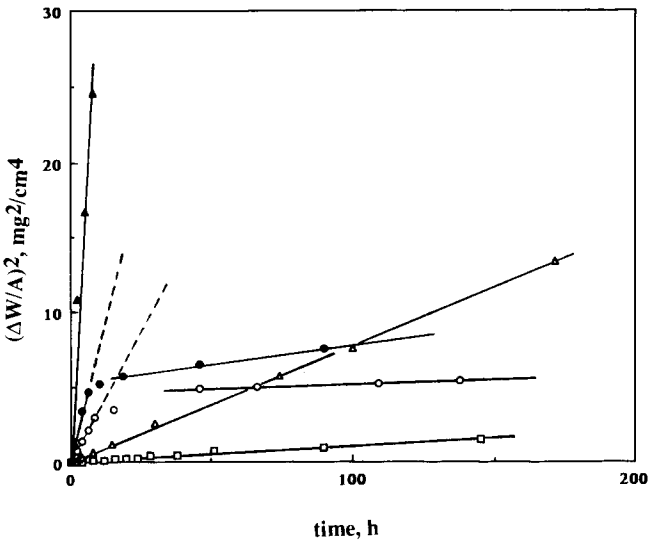

Fig. 7. Parabolic plot of weight change for TiN-reinforced Si/6/3 composite oxidized at various temperatures in air. □, 950°C; △, 1100°C; ○, 1250°C; ●, 1325°C; ▲, 1400°C.

considering the structural perfection of TiO_2, a nonstoichiometric composition with oxygen vacancies is generally preserved. The transportation of oxygen in TiO_2 layer is thermodynamically preferred compared to that of Ti ions due to the existence of these oxygen vacancies. Inward diffusion of oxygen through the TiO_2 layers is thus favorable and faster than the outward diffusion of Ti ion. As a result, the oxidation reaction is more likely to occur at the interface between the outer TiO_2 layer and TiN-depleted zone, that is, $SiO_2 + TiO_2$ thin layer.

3.2 TiN reinforced Si/6/3 composite

In the case of TiN-reinforced Si/6/3 composite, the oxidation behavior is slightly different from that of TiN-reinforced Si/4/0 composite. Figure 7 shows the

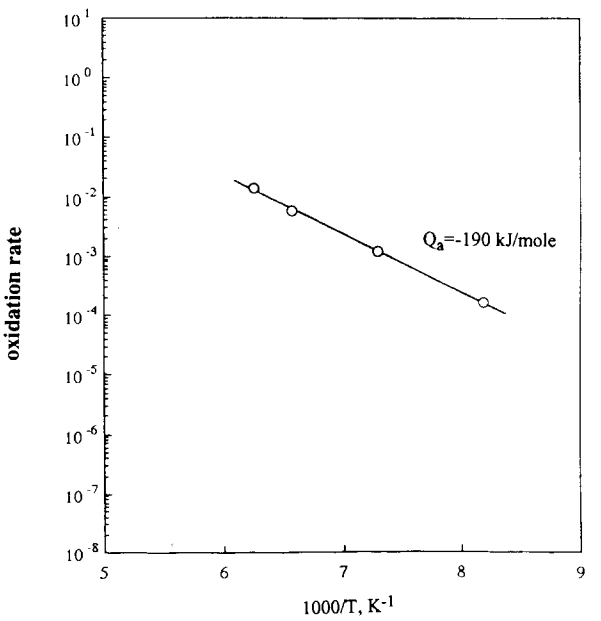

Fig. 8. Arrhenius plot of oxidation rate constant for TiN-reinforced Si/6/3 composites oxidized in air.

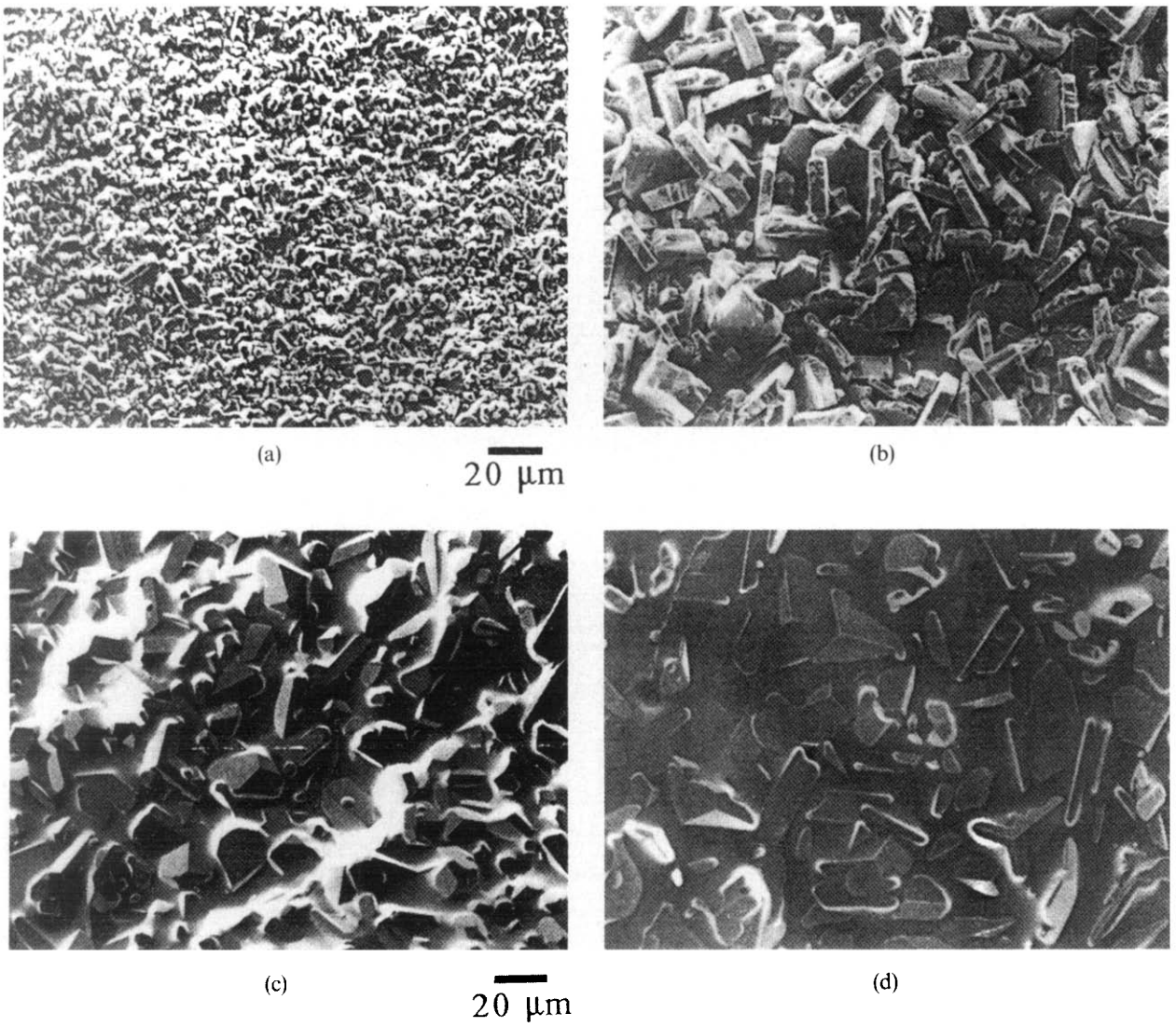

Fig. 9. Surface morphologies of TiN-reinforced Si/6/3 composite exposed at (a) 950, (b) 1100, (c) 1250 and (d) 1325°C in air for 175 h.

parabolic plots (squares of the weight gain per unit area versus time) of TiN-reinforced Si/6/3 composite oxidized at temperatures ranging from 950 to 1400°C in air. For specimens tested at 950 and 1100°C, all the data can fit into straight lines. However, at 1250 and 1325°C, two linear regions are found. A break on the parabolic plot is observed at $t \approx 10$–15 h of exposure. This indicates that different rate-controlling mechanisms were active after longer exposure. A slower oxidation rate was observed for the second linear region.

Figure 8 shows the plot of the initial parabolic rate constant versus $1/T$ for TiN-reinforced Si/6/3 composite. It was found that the initial parabolic rate constant fell into a straight line with an apparent activation energy of 190 kJ/mol which is very close to that for the oxidation of the TiN-reinforced Si/4/0 composite. The surface morphologies of the TiN-reinforced Si/6/3 composite exposed at 950 and 1100°C in air for 175 h is shown in Fig. 9(a) and (b). It is clear that the surface was also covered by rod- or plate-like titanium dioxide (TiO_2, rutile) as that in the TiN-reinforced Si/4/0 specimen. The size of these crystallites also increases as the exposure temperature increases. As a result, the oxidation behavior of TiN-reinforced Si/6/3 composite up to 1100°C is believed to be governed by the same oxidation reaction and rate-controlling mechanism as that for the TiN-reinforced Si/4/0 composite.

At 1250 and 1325°C, however, a different morphology was observed on the surfaces of the oxidized TiN-reinforced Si/6/3 composites, as shown in Fig. 9(c) and (d). In this case, the surface of the oxidized specimens was covered by a film-like layer accompanied with TiO_2 crystallites. These TiO_2 crystallites were isolated instead of stacking on each other as in the case of TiN-reinforced Si/4/0 composite exposed at the same temperatures. Figure 10 shows the backscattered electron image (BEI) of a transverse section of the TiN-reinforced Si/6/3 composite exposed at 1250°C for 175 h. Three distinct zones similar to those in the oxidized Si/4/0 specimen were also clearly observed. The results of EPMA element line scanning across this oxide scale is shown in Fig. 11. The outer oxide layer appears to be composed of

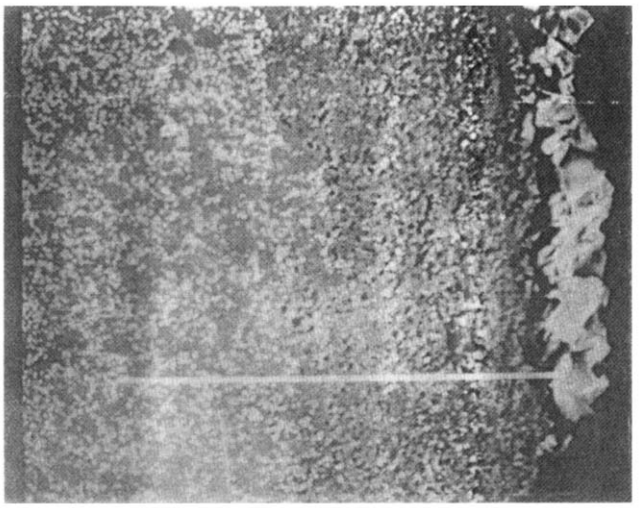

Fig. 10. The back-scattered electron image (BEI) of a transverse section of the TiN-reinforced Si/6/3 composite oxidized at 1250°C for 175 h. Three distinct zones can be observed: external oxide layer, TiN-depleted zone and bulk material.

TiO_2 and amorphous silica (X-ray analysis of the oxide scale showed only TiO_2 diffraction pattern). A higher concentration of Al than that in the bulk material was detected in the oxide layer. This strongly suggests that Al_2O_3 was involved in the formation of this amorphous silica layer. However, the observation of TiN-depleted zone indicated that the oxidation of TiN is still the primary oxidation reaction and the outward diffusion of Ti to the oxide scale was faster than the inward diffusion of oxygen. The change of oxidation behaviour of the TiN-reinforced Si/6/3 composite at 1250 and 1325°C may be related to the nature of the sintering additives, which in turn, will affect the nature of the intergranular phases. Further work is in progress to define the role of the liquid phase on the oxidation behaviour of alumina-containing composites.

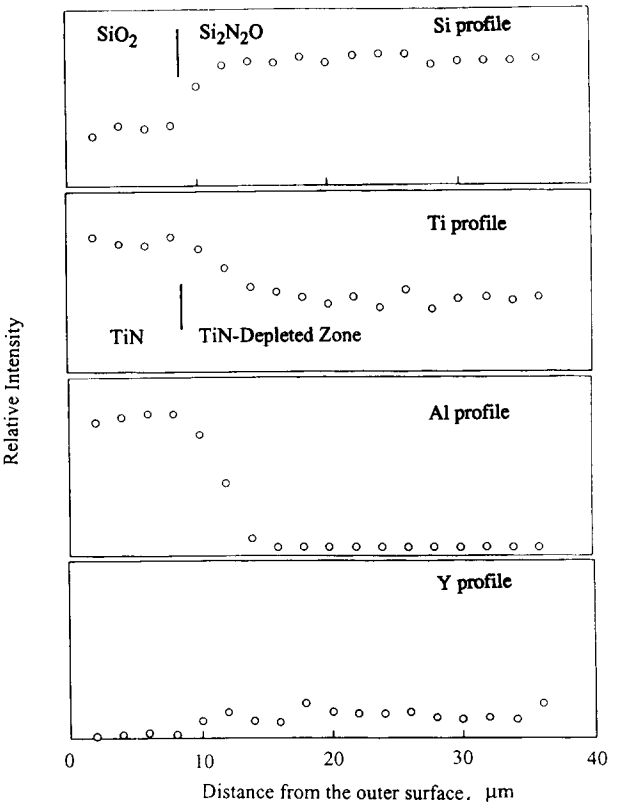

Fig. 11. EPMA element line scan (across the oxide scale) of the TiN-reinforced Si/6/3 composite exposed at 1250°C for 175 h.

Another important factor to be taken into account for the oxidation of TiN–Si_2N_2O composites is the evolution of nitrogen in the oxidation of TiN. TiN is believed to decompose first before the Ti ion can diffuse to the surface oxide scale. N_2 is expected to nucleate at the interface of TiN-depleted zone and bulk material and diffuse outwards to the surface. If the oxidation rate is too high, N_2 bubbles will be formed at this interface due to the build up of high nitrogen pressure. Figure 12 shows the transverse section of the TiN-reinforced Si/6/3 composite

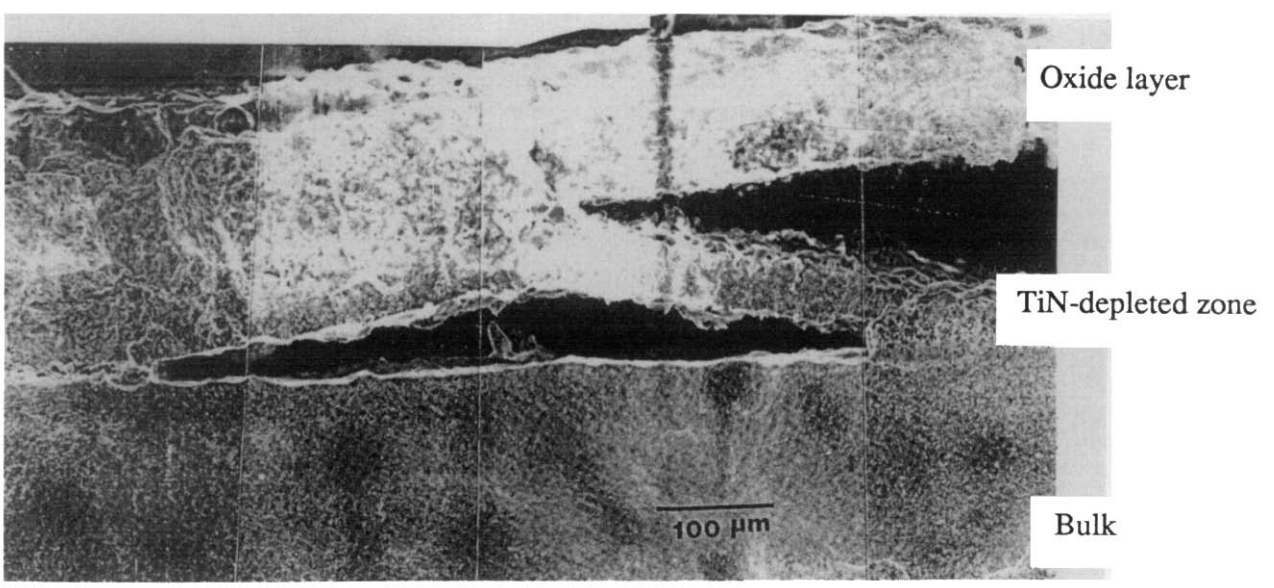

Fig. 12. A cross-section of the TiN-reinforced composite exposed at 1400°C for 48 h.

exposed at 1400°C for only 48 h. Bubbles were clearly observed near the TiN depleted zone–bulk material interface. Another interesting feature found in this figure is that the thickness of TiN-depleted zone and the oxide layer near these bubbles ($\sim 120\,\mu$m) is smaller than that without bubbles ($\sim 200\,\mu$m). Obviously, the formation of these bubbles would block the diffusion route of Ti to the oxide layer and thus reduce the further oxidation at these areas. However, when the nitrogen pressure within these bubbles exceeds a critical value, cracking (or exfoliation) of the oxide layer might occur and thus speed up the oxidation rate again.

4 Summary

(1) The thermal stability of TiN–Si_2N_2O composites is dominated by the oxidation of TiN phase.

(2) For TiN-reinforced Si/4/0 composite, the oxidation follows the classic parabolic behavior with an activation energy of 194 kJ/mol at temperatures ranging from 950 to 1400°C. The oxide scale consists of TiO_2 only. The inward diffusion of oxygen through the TiO_2 layer is postulated to be the oxidation rate-governing step.

(3) For the TiN-reinforced Si/6/3 composite, a transition temperature, T_c, was found separating two different oxidation behaviors. For $T \leq 1100$°C, the oxide scale and apparent activation energy were found to be comparable with those of the TiN-reinforced Si/4/0 composite. A mechanism similar to that of TiN-reinforced Si/4/0 composite is believed to control the oxidation behavior at this temperature range. For $T \geq 1250$°C, the oxide scale is composed of TiO_2 from the oxidation of TiN and amorphous SiO_2 from the oxidation of Si_2N_2O. The outward diffusion of Ti ions through this oxide layer ($SiO_2 + TiO_2$) appears to be the rate-determining mechanism.

Acknowledgements

This work was partially supported by the National Science Foundation through the Presidential Young Investigator Award to J.-M. Yang (DDM 9057030) and Electric Power Research Institute (Dr W. Bakker is the project monitor). The authors also thank Mr C. J. Shih and A. Ezis at Cercom Inc. for their technical support.

References

1. Ohashi, M., Tabata, H. & Tanzaki, S., High-temperature flexural strength of hot-pressed silicon oxynitride ceramics. *J. Mat. Sci. Lett.*, **7** (1988) 339–40.
2. Huang, Z. K., Greil, P. & Petzow, G., Formation of silicon oxynitride from Si_3N_4 and SiO_2 in the presence of Al_2O_3. *Ceram. Int.*, **10**(1) (1984) 14–17.
3. Billy, M., Boch, P., Dumazeau, C., Glandus, J. C. & Goursat, P., Preparation and properties of new silicon oxynitride based ceramics. *Ceram. Int.*, **7**(1) (1981) 13–18.
4. Aveston, J., Strength and toughness in fiber-reinforced ceramics. in *The Properties of Fiber Composites: Conference Proceedings*. National Physical Laboratory, UK, 1971, pp. 15–27.
5. Rice, R. W., Mechanisms of toughening in ceramic matrix composites. *Ceram. Eng. Sci. Proc.*, **2**(7–8) (1978) 694–714.
6. Donald, I. W. & McMillan, P. W., Review: ceramic matrix composites. *J. Mater. Sci.*, **11** (1976) 949–72.
7. Yasutomi, Y. & Sobue, M., Development of reaction-bonded electro-conductive TiN–Si_3N_4 and resistive Al_2O_3–Si_3N_4 composites. *Ceram. Eng. Sci. Proc.*, **11**(7–8) (1990) 857–67.
8. Jiang, D. L., Wang, J. H., Li, Y. L. & Ma, L. T., Studies on the strengthening of silicon carbide-based multiphase ceramics. I: the SiC–TiC system. *Mat. Sci. Eng.*, **A109** (1991) 401–6.
9. Martin, C., Cales, B. & Mathieu, P., Electrical discharge machinable ceramic composites. *Mat. Sci. Eng.*, **A109** (1989) 351–6.
10. Jimbou, R., Takahashi, K., Matsushita, Y. & Kosugi, T., SiC–ZrB_2 electroconductive ceramic composite. *Adv. Ceram. Mater.*, **1**(4) (1986) 341–5.
11. McMurty, C. H., Boecker, W. D. G., Seshardri, S. G., Zanghi, J. S. & Garnier, J. E., Microstructure and material properties of SiC–TiB_2 particulate composites. *Am. Ceram. Soc. Bull.*, **66**(2) (1987) 325–9.
12. Gadalla, A. M. & Petrofes, N. F., Surface of advanced ceramic composites formed by electrical discharge machining. *Mater. Manuf. Process.*, **5**(2) (1990) 253–71.
13. Lin, W., Yang, J.-M., Ting, S.-J., Azis, A. & Shih, J., Processing and microstructural development of in situ TiN-reinforced silicon nitride/silicon oxynitride composites. *J. Am. Ceram. Soc.*, **75** (1992) 2945–52.
14. Bellosi, A., Tampieri, A. & Liu, Yu-Zhen, Oxidation behavior of electroconductive Si_3N_4–TiN composites. *Mat. Sci. Eng.*, **A127** (1990) 115–22.
15. Mukerji, J. & Biswas, S. K., Synthesis, properties, and oxidation of alumina titanium nitride composites. *J. Am. Ceram. Soc.*, **73**(1) (1990) 142–5.
16. Munster, A. & Schlamp, G., Oxidation of titanium nitride: I and II. *Z. Physik. Chem. (Frankfort)*, **13** (1957) 59–94.
17. Jenkins, A. E., A further study of the oxidation of titanium and its alloys at elevated temperatures. *J. Inst. Metals*, **84**(1) (1955) 1–9.